Robust Quadrotor Attitude Control Using Incremental Nonlinear Dynamic Inversion for External Disturbances and Model Mismatches

Limin Ouyang, Yuan Fang, Yuyun Xia and Yinghong Tian

***Abstract*—External disturbances and model mismatches pose significant challenges to the robust control of existing quadcopter Unmanned Aerial Vehicle (UAV) controllers. This article proposes a quadcopter control algorithm that integrates Incremental Nonlinear Dynamic Inversion (INDI) to address these issues. The algorithm consists of a Nonlinear Dynamic Inversion (NDI)-based outer loop controller and an INDI-based inner loop controller. Compared to traditional PID controllers, the proposed algorithm utilizes feedback data such as angular acceleration and motor speed to allocate incremental control torques, and employs magnetic encoders for closed-loop control of motor speed. Experiments were conducted both on a MATLAB simulation platform and an actual UAV. The results demonstrate that INDI outperforms PID in suppressing disturbances and handling model mismatches, confirming its control effectiveness and robustness.**

***Index Terms*—Quadrotor, Attitude Control, INDI, NDI, External Disturbances, Model Mismatches**

I. Introduction

In recent years, quadcopter Unmanned Aerial Vehicle (UAV) have been frequently deployed in civil, industrial, agricultural, military, and rescue application [1], [2]. In some of these fields, UAVs are required to perform highly complex and fast-paced tasks, which demand high performance from their controllers. Specifically, for UAVs executing complex missions, disturbance rejection and handling model mismatches are critical criteria. The purpose of this article is to design a controller to enhance these capabilities.

To control quadcopter UAVs, scholars have proposed many control methods based on linearization such as PID(proportion-integration-differentiation) [3], LQR (Linear Quadratic Regulator) [4], [5], H_∞ control [6], [7]. However, linearized controllers do not control well in the face of high-speed or large-angle maneuvers because the nonlinearity of the quadrotor has been non-negligible in these cases, which is a drawback of linear controllers. The reason for this is that UAV flight is subject to uncertainties in body torque due to factors such as higher-order aerodynamic effect, center of gravity deviations, different motor rotor blades, etc. Difficulty in modeling aerodynamic drag is also a major reason for the inability to linearize the flight system, and thus dealing with these issues poses an important challenge to the control design.

To address this issue, researchers have proposed various nonlinear controllers, such as backstepping control , sliding mode control , nonlinear model predictive control , and even neural network-based controllers [8], [9], [10], [11], [12]. These control methods undoubtedly achieve good performance but also increase the complexity and design difficulty of the control system. Additionally, these control methods are challenging to quickly transplant and apply to other quadrotor platforms.

Therefore, a control method based on Nonlinear Dynamic Inversion (NDI) is proposed, aiming to linearize the control system [13]. NDI uses an aerodynamic model approach to linearize the quadrotor's dynamics, heavily relying on the accuracy of the aerodynamic model. Consequently, NDI performs poorly when dealing with model mismatches [14].

Due to criticism of the NDI method for its heavy reliance on accurate models, researchers have proposed an improved form of NDI, known as Incremental Nonlinear Dynamic Inversion (INDI) [15], [16], [17]. INDI offers better robustness and lower model dependence than NDI [18]. Although INDI is described as an improved version of NDI, the two are based on very different design principles. INDI aims to mitigate the adverse effects of model mismatches by measuring dynamic quantities of the system, continuously measuring and correcting errors [19], [20]. This approach reduces reliance on the system model, enhancing the stability and robustness of the closed-loop control system[21], [22], [23]. Its effectiveness has been confirmed in [24].

The main contributions of this article are as follows:s

1). The design of a controller based on NDI and INDI, which counteract the nonlinearity issues of quadcopter systems and improves disturbance rejection and adaptability to model mismatches.

2). Compared to the traditional method of directly controlling ESCs to manage motor speed, we use magnetic encoders attached to the bottom of the motors for precise motor speed control, thereby achieving more accurate torque control.

The main structure of this article is as follows:

Manuscript received July 7, 2024; revised February 4, 2025.

Limin Ouyang is a graduate student in the school of Communication and Electronic Engineering, East China Normal University, Shanghai, China. (email:51255904058@stu.ecnu.edu.cn)

Yuan Fang is a graduate student in the school of Communication and Electronic Engineering, East China Normal University, Shanghai, China. (email: 51255904057@stu.ecnu.edu.cn)

Yuyun Xia is a graduate student in the school of Communication and Electronic Engineering, East China Normal University, Shanghai, China. (email: 51215904079@stu.ecnu.edu.cn)

Yinghong Tian is an associate professor in the school of Communication and Electronic Engineering, East China Normal University, Shanghai, China. (email: yhtian@cee.ecnu.edu.cn)

In Section II we introduce the modeling of the quadrotor and the theoretical derivation of INDI. Section III introduces the proposed controller. Section IV shows the simulation of the proposed controller and the actual flight effect of the proposed controller. The conclusion is shown in section V.

II. PRELIMINARIES

A. Quadrotor Model

A 6-degree-of-freedom quadrotor is shown in Fig. 1. The modeling equation for the quadrotor is:

$$\mathbf{J}\dot{\mathbf{\Omega}} + \mathbf{\Omega} \times \mathbf{J}\mathbf{\Omega} = \boldsymbol{\mu} + \boldsymbol{\mu}_{\mathbf{e}}. \tag{1}$$

Where $\mathbf{J}$={Jx,Jy,Jz} is the inertia matrix of the system, $\mathbf{\Omega}$ is the angular velocity of the airframe, $\dot{\mathbf{\Omega}}$ is the angular acceleration of the airframe, and $\boldsymbol{\mu}$ represents the control moment vector, derived from the power of the UAV rotor. $\boldsymbol{\mu}_{\mathbf{e}}$ is the disturbance moment, which is derived from factors such as air resistance, model bias, rotor variance, and so on [25].

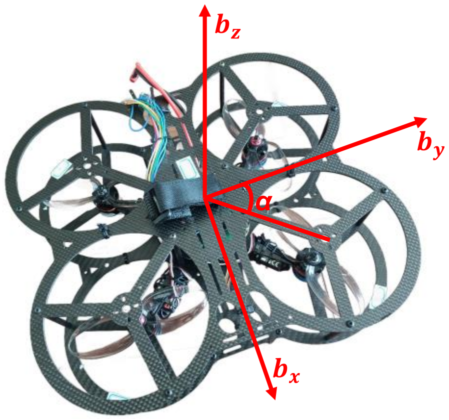

Fig. 1. UAV and reference system of body.

Here, $\boldsymbol{\mu}_{\mathbf{e}}$ is a quantity that is difficult to model accurately, yet its effect cannot be ignored, introducing instability to the system as well as reducing its robustness, so in the next section, we will introduce the INDI method to eliminate the harmful effects of this item.

The total thrust T and the control moment vector $\boldsymbol{\mu}$ are given by:

$$\begin{bmatrix} T \\ \boldsymbol{\mu} \end{bmatrix} = \mathrm{G}_1 \boldsymbol{\omega}^{\circ 2} + \mathrm{G}_2 \dot{\boldsymbol{\omega}}. \tag{2}$$

Where $\boldsymbol{\omega}$ is the vector of angular rates of each propeller, $^\circ$ indicates the Hadamard power, G_1 is the manipulation efficiency matrix of the system, defined as:

$$G_1 = \mathrm{c_T} \times \begin{bmatrix} 1 & 1 & 1 & 1 \\ \mathrm{d}\sin\alpha & -\mathrm{d}\sin\alpha & -\mathrm{d}\sin\alpha & \mathrm{d}\sin\alpha \\ -\mathrm{d}\cos\alpha & -\mathrm{d}\cos\alpha & \mathrm{d}\cos\alpha & \mathrm{d}\cos\alpha \\ \mathrm{c_M}/\mathrm{c_T} & -\mathrm{c_M}/\mathrm{c_T} & \mathrm{c_M}/\mathrm{c_T} & -\mathrm{c_M}/\mathrm{c_T} \end{bmatrix}. \tag{3}$$

Where $\mathrm{c_T}$ is the rotor thrust coefficient, $\mathrm{c_M}$ is the rotor torque coefficient, d is the distance from the center of the motor rotor to the center of gravity of the body, α is shown in Fig. 1.

G_2 matrix is defined as:

$$G_2 = \begin{bmatrix} 0 & 0 & 0 & 0 \\ 0 & 0 & 0 & 0 \\ 0 & 0 & 0 & 0 \\ \mathrm{I_r} & -\mathrm{I_r} & \mathrm{I_r} & -\mathrm{I_r} \end{bmatrix}. \tag{4}$$

Where $\mathrm{I_r}$ is the moment of inertia of the rotor.

The $\mathrm{G}_2\dot{\boldsymbol{\omega}}$ term is the torque due to the angular acceleration of the rotor, and in this article, we will use the INDI approach to eliminate the effect of the inertial torque term G_2.

B. Nonlinear Dynamic Inversion

Given such a multi-input, multi-output nonlinear system:

$$\dot{\boldsymbol{x}} = \mathrm{f}(\boldsymbol{x}) + \mathrm{g}(\boldsymbol{x})\boldsymbol{u}. \tag{5}$$

$$\boldsymbol{y} = \mathrm{h}(\boldsymbol{x}). \tag{6}$$

Where $\boldsymbol{x}$ is the state vector of the system, $\boldsymbol{u}$ is the input vector of the system, $\boldsymbol{y}$ is the output vector of the system, $\boldsymbol{x}$ and $\boldsymbol{y}$ have the same dimension.

Derivation of $\boldsymbol{y}$:

$$\dot{\boldsymbol{y}} = \frac{\partial \mathrm{h}}{\partial \mathrm{x}}\dot{\boldsymbol{x}} = \frac{\partial \mathrm{h}}{\partial \mathrm{x}}(\mathrm{f}(\boldsymbol{x}) + \mathrm{g}(\boldsymbol{x})\boldsymbol{u}) = \mathrm{F}(\boldsymbol{x}) + \mathrm{G}(\boldsymbol{x})\boldsymbol{u}. \tag{7}$$

The $\mathrm{G}(\boldsymbol{x})$ matrix must be invertible, replace $\dot{\boldsymbol{y}}$ with an implicit input $\boldsymbol{v}$, and flip the above equation to obtain the dynamic control inverse:

$$\boldsymbol{u} = G(\boldsymbol{x})^{-1}(\boldsymbol{v} - \mathrm{F}(\boldsymbol{x})). \tag{8}$$

In this way the nonlinear system is transformed into a linear system using nonlinear dynamic feedback, and then linear control methods can be applied to accomplish the control of the system.

C. Incremental Nonlinear Dynamic Inversion

For such a typical nonlinear system:

$$\dot{\boldsymbol{x}} = \mathrm{f}(\boldsymbol{x}, \boldsymbol{u}). \tag{9}$$

Unlike NDI, there is no need to flip the entire system dynamics, (9) in here Taylor unfolds at $\boldsymbol{x}_0$ and $\boldsymbol{u}_0$, where $\boldsymbol{x}_0$ is the state quantity at the current moment and $\boldsymbol{u}_0$ is the input quantity at the current moment.

$$\dot{\boldsymbol{x}} = \mathrm{f}(\mathrm{x}_0, \mathrm{u}_0) + \frac{\partial f(x,u)}{\partial x}\Big|_{x=x_0, u=u_0}(\boldsymbol{x} - \boldsymbol{x}_0) + \frac{\partial f(x,u)}{\partial u}\Big|_{x=x_0, u=u_0}(\boldsymbol{u} - \boldsymbol{u}_0) + \Delta. \tag{10}$$

If the sampling interval is short enough, the input quantity $\boldsymbol{u}$ changes much faster than the system state quantity $\boldsymbol{x}$. That is, in satisfying a short enough time $\boldsymbol{x} \approx \boldsymbol{x}_0$, $\boldsymbol{u} \neq \boldsymbol{u}_0$ the above equation can be simplified as:

$$\dot{\boldsymbol{x}} = \dot{\boldsymbol{x}_0} + \boldsymbol{G}(\boldsymbol{x}_0, \boldsymbol{u}_0)(\boldsymbol{u} - \boldsymbol{u}_0). \tag{11}$$

Similarly, we replace $\dot{\boldsymbol{x}}$ with an implicit output $\boldsymbol{v}'$,The expression for the control quantity $\boldsymbol{u}$ is then obtained:

$$\boldsymbol{u} = \boldsymbol{u}_0 + \boldsymbol{G}(\boldsymbol{x}_0, \boldsymbol{u}_0)^{-1}(\boldsymbol{v}' - \dot{\boldsymbol{x}_0}). \tag{12}$$

Where $\boldsymbol{v}'$ can be thought of as a derivative of the desired output, $\dot{\boldsymbol{x}_0}$ is a derivative of the current state. $\boldsymbol{G}(\boldsymbol{x}_0, \boldsymbol{u}_0)$ is an invertible matrix, and the increment of the input is $\boldsymbol{u} - \boldsymbol{u_0}$.

III. METHTODOLOGIES

For attitude control of a quadrotor UAV, the relationship between the Euler angle $\boldsymbol{\zeta}$={ϕ, θ,ψ } to angular velocity $\boldsymbol{\Omega}$ is represented by the following:

$$\dot{\boldsymbol{\zeta}} = \mathrm{R}\boldsymbol{\Omega}\,. \tag{13}$$

$$\mathrm{R}=\begin{bmatrix}1 & tan\theta sin\phi & tan\theta cos\phi \\ 0 & cos\phi & -sin\phi \\ 0 & sin\phi/cos\theta & cos\phi/cos\theta\end{bmatrix}. \tag{14}$$

It can be seen that the relationship from Euler angle to angular velocity is nonlinear, which is particularly noticeable in the case of a quadrotor with a large deflection angle. The system is linearized using the NDI approach:

$$\boldsymbol{u}_\Omega = R^{-1}\boldsymbol{v}_\zeta\,. \tag{15}$$

$$\boldsymbol{v}_\zeta = \boldsymbol{K}_\zeta e = \begin{bmatrix}k_1(\phi_\mathrm{d} - \phi_\mathrm{r}) \\ k_2(\theta_\mathrm{d} - \theta_\mathrm{r}) \\ k_3(\psi_\mathrm{d} - \psi_\mathrm{r})\end{bmatrix}. \tag{16}$$

Where $\{\phi_d, \theta_d, \psi_d\}$ is the desired Euler angle, $\{\phi_\mathrm{r}, \theta_\mathrm{r}, \psi_\mathrm{r}\}$ is the reference angle, $\boldsymbol{u}_\Omega$ is the input to the system in this case the input angular velocity. $\boldsymbol{K}_\zeta = \{\mathrm{k}_1, \mathrm{k}_2, \mathrm{k}_3\}$ is the Gain according to the actual performance of the system.

After getting the input angular velocity, we can subtract it from the reference angular velocity of the system to obtain the desired angular acceleration:

$$\dot{\boldsymbol{\Omega}}_\mathrm{d} = \boldsymbol{K}_\Omega(\boldsymbol{u}_\Omega - \boldsymbol{\Omega}_\mathrm{ref}). \tag{17}$$

The next step is to track the angular acceleration command using the INDI. Considering the effect of the unmodeled term $\boldsymbol{\mu}_\mathrm{e}$ in (1), we rewrite (1):

$$\boldsymbol{\mu}_\mathrm{e} = \mathbf{J}\dot{\boldsymbol{\Omega}}_\mathrm{ref} + \boldsymbol{\Omega}_\mathrm{ref} \times \mathbf{J}\boldsymbol{\Omega}_\mathrm{ref} - \boldsymbol{\mu}_\mathrm{ref}. \tag{18}$$

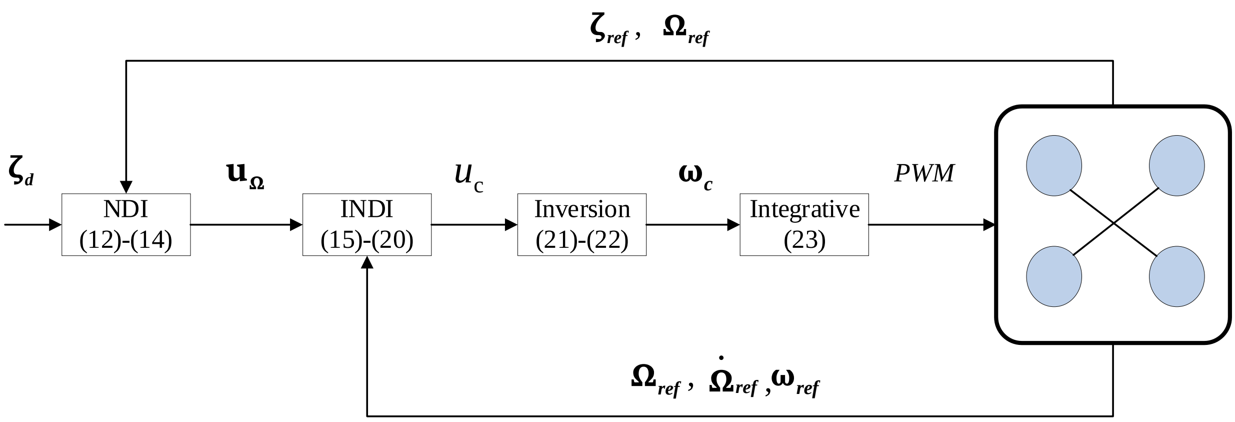

Fig. 2. Control diagram of the NDI, combined with an INDI inner loop controller.

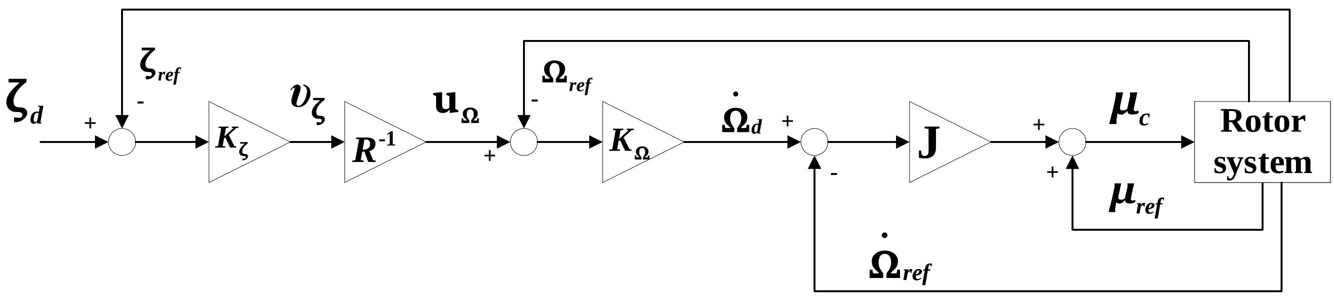

(a) Acceleration and attitude control

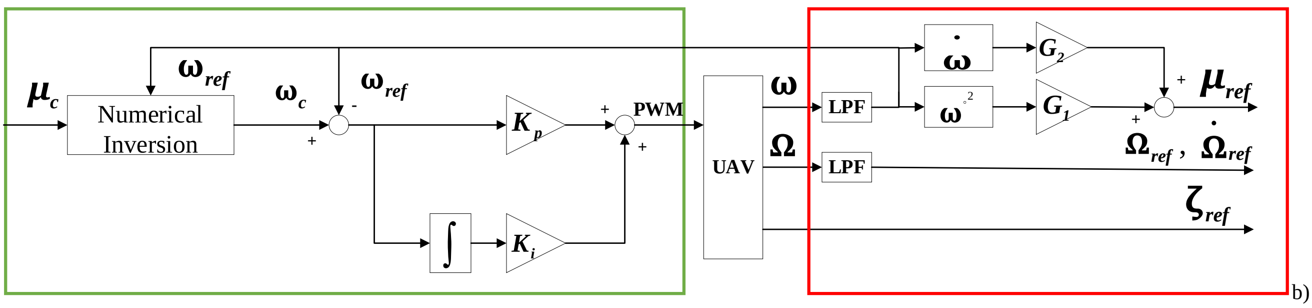

(b) Rotor system control

Fig. 3. The detailed structure diagram of system control

$\boldsymbol{\mu}_{\text{ref}}$ is the current torque generated by the motor rotor, after we obtain the rotor speed values, we can use (2) to calculate this value. $\boldsymbol{\Omega}_{\text{ref}}$ and $\dot{\boldsymbol{\Omega}}_{\text{ref}}$ represent the current angular velocity and angular acceleration, respectively.

Then:

$$\begin{aligned}\dot{\boldsymbol{\Omega}}_{\text{d}} &= \mathbf{J}^{-1}\,(\boldsymbol{\mu}_{\text{c}} + \boldsymbol{\mu}_{\text{e}} - \boldsymbol{\Omega}\times\mathbf{J}\boldsymbol{\Omega}) \\ &= \mathbf{J}^{-1}\,(\boldsymbol{\mu}_{\text{c}} + (\mathbf{J}\dot{\boldsymbol{\Omega}}_{\text{ref}} - \boldsymbol{\mu}_{\text{ref}} + \boldsymbol{\Omega}_{\text{ref}}\times\mathbf{J}\boldsymbol{\Omega}_{\text{ref}}) - \boldsymbol{\Omega}\times\mathbf{J}\boldsymbol{\Omega}).\end{aligned} \tag{19}$$

The change in angular acceleration is so much faster than the change in angular velocity over a very short sampling interval, and the change in angular velocity is negligible compared to the change in angular acceleration and control torque, thus simplifying (19):

$$\dot{\boldsymbol{\Omega}}_{\text{d}} = \dot{\boldsymbol{\Omega}}_{\text{ref}} + \mathbf{J}^{-1}(\boldsymbol{\mu}_{\text{c}} - \boldsymbol{\mu}_{\text{ref}}). \tag{20}$$

And the new control torque $\boldsymbol{\mu}_{\text{c}}$:

$$\boldsymbol{\mu}_{\text{c}} = \boldsymbol{\mu}_{\text{ref}} + \mathbf{J}\times(\dot{\boldsymbol{\Omega}}_{\text{d}} - \dot{\boldsymbol{\Omega}}_{\text{ref}}). \tag{21}$$

After getting $\boldsymbol{\mu}_{c}$, We use (2) to inversely solve for the speed of the motor:

$$\begin{bmatrix} T \\ \boldsymbol{\mu}_{\text{c}} \end{bmatrix} = \mathrm{G}_1\boldsymbol{\omega}_{\text{c}}^{\circ 2} + \mathrm{G}_2\dot{\boldsymbol{\omega}}_{c}\,. \tag{22}$$

Finally, the throttle ***PWM*** value input to the Electronic Speed Controller (ESC) is:

$$\boldsymbol{PWM} = \boldsymbol{K}_{\text{p}}(\boldsymbol{\omega}_{\text{c}} - \boldsymbol{\omega}_{\text{ref}}) + \boldsymbol{K}_{\text{i}}\int(\boldsymbol{\omega}_{\text{c}} - \boldsymbol{\omega}_{\text{ref}})\text{dt}. \tag{23}$$

TABLE I
OVERVIEW OF CONTROL COMPONENTS

Component	Method	Reference	Output
Outer loop Control	NDI	$\boldsymbol{\zeta}_{\text{d}}, \boldsymbol{\zeta}_{\text{ref}}$	$\boldsymbol{u}_{\Omega}$
Inner loop Control	INDI	$\boldsymbol{u}_{\Omega}, \boldsymbol{\Omega}_{\text{ref}}, \dot{\boldsymbol{\Omega}}_{\text{ref}}, \boldsymbol{\mu}_{\text{ref}}$	$\boldsymbol{\mu}_{\text{c}}$
Actuator And Rotor Control	Inversion	$\boldsymbol{\mu}_{\text{c}}$	$\boldsymbol{\omega}_{\text{c}}$
Rotor Speed Control	Integrative	$\boldsymbol{\omega}_{\text{ref}}$	***PWM***

The general control block diagram is shown in Fig. 2, and the detailed control block diagram is shown in Fig. 3. Fig. 2 shows a general control strategy. Fig. 3 refines the mathematical relationship in the control method.

IV. Implementation

We used Matlab simulations and real airplane flights to verify the algorithm's effectiveness. The results prove that the INDI inner-loop controller outperforms the serial PID controller [3].

Before starting the experiment, we introduce the design and implementation details of our simulation platform and real flight. The PID and INDI are run in a Matlab simulation system. We built a power unit model: to realize the function of getting the motor speed from the throttle value; a control efficiency model: to realize the function of getting the combined lift force and three-axis moments from the motor speed; and an attitude dynamics model: to realize the function of getting the angular acceleration, angular velocity, and attitude angle from the moments. The parameters of the simulated quadcopter are listed in TABLE II. The parameters of the simulator are measured by the real aircraft to ensure the maximum consistency between the simulated and real environments.

TABLE II
AIRFRAME PARAMETERS OF THE AIRCRAFT

Parameters	Values
mass[kg]	0.852
J [kg × m^2]	Diag (6.051e-3,6.131e-3,7.072e-3)
d[m]	0.11
α[deg]	45
c_T [N/(rad/s)^2]	1.084 × 1e-6
c_M [N×m/(rad/s)^2]	1.574 × 1e-8

The simulation step of Matlab software is 0.001s, and it operates at a frequency of 1000Hz. In real-world flight, the IMU data is updated at a rate of 200Hz, the rotor speed is updated at a rate of 400Hz by a motor equipped with a magnetic encoder. The NDI operates at a frequency of 200Hz, and the inner loop of the INDI operates at a frequency of 400Hz, and the closed-loop control of rotor speed is also at a rate of 400Hz. The PID controller maintains the same control frequency.

A. Simulation Test

1)、Inner loop angular velocity control

In this simulation experiment, the control effect of the proposed INDI controller was first tested. The flight performance of quadcopter UAVs is largely determined by the control effect of angular velocity, so the angular velocity control effect of INDI control was tested here.

The step response of angular velocity under the proposed controller demonstrates excellent performance, reaching the set value of 1 rad/s within approximately 0.5 seconds in Fig. 4(a). As shown in Fig. 4(b), the blue line represents the set angular velocity reference value, while the orange line depicts the actual angular velocity performance. The INDI controller exhibits a favorable tracking response.

2)、Outer loop angle control

After achieving satisfactory angular velocity control performance, and integrating the outer loop NDI controller, the overall attitude control effectiveness is tested.

Fig. 5(a) demonstrates the effectiveness of the proposed controllers, indicating the efficacy of INDI. Subsequently, step responses were separately tested for the cascaded PID and the proposed controller integrating INDI. A comparison was made between the INDI controller and a tuned PID controller in Fig. 5(b). In an ideal simulation environment, the performance of cascaded PID and INDI is almost identical. The difference between the two is reflected in the subsequent robustness test. These tests assess how each controller performs under different operating conditions and disturbances, which are more representative of real-world scenarios. The results revealed that while both controllers exhibit good performance in the ideal case, the INDI controller demonstrates significantly higher robustness.

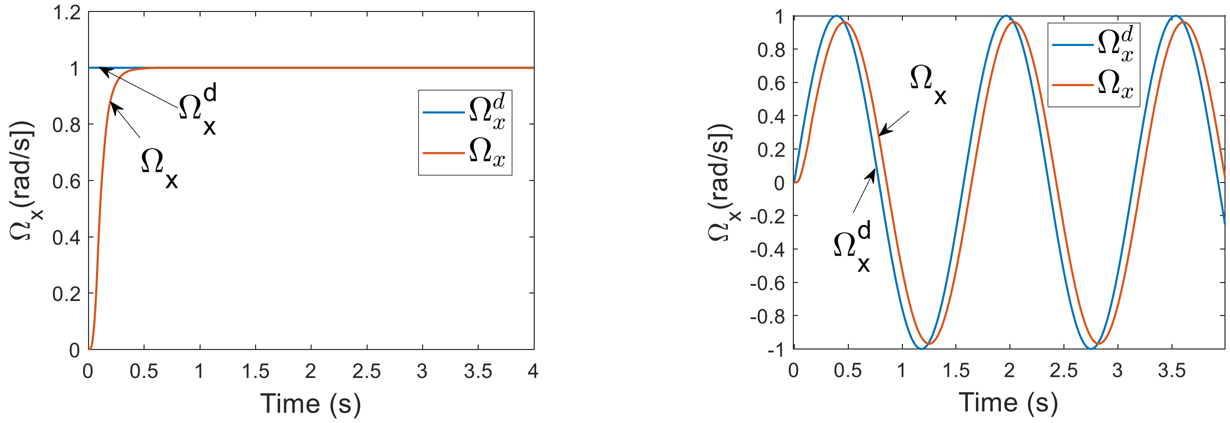

(a) Step response of angular velocity under the INDI control scheme (b) Angular velocity tracking response

Fig. 4. Step response and tracking response under the INDI control scheme.

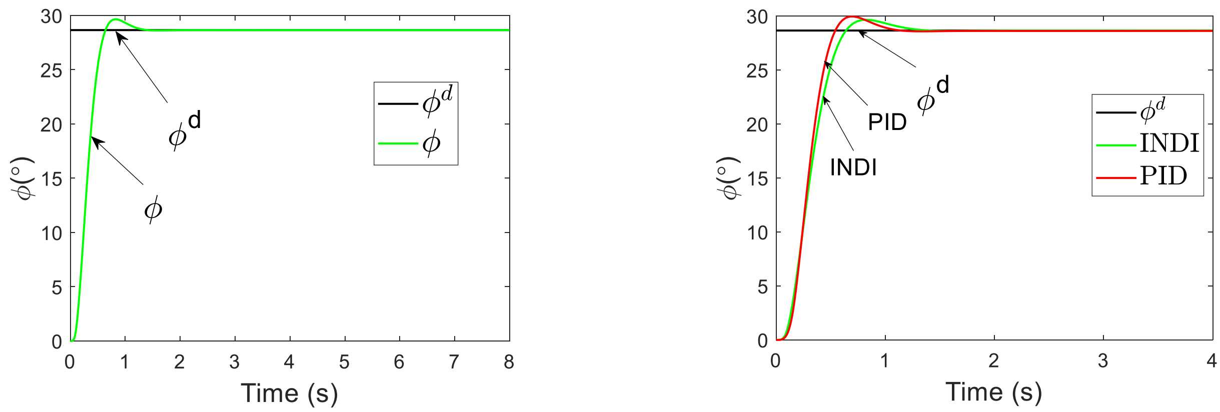

(a) Step response of attitude under INDI & NDI controllerss (b) Comparison of step responses between INDI and PID

Fig. 5. The performance effect of two kinds of control

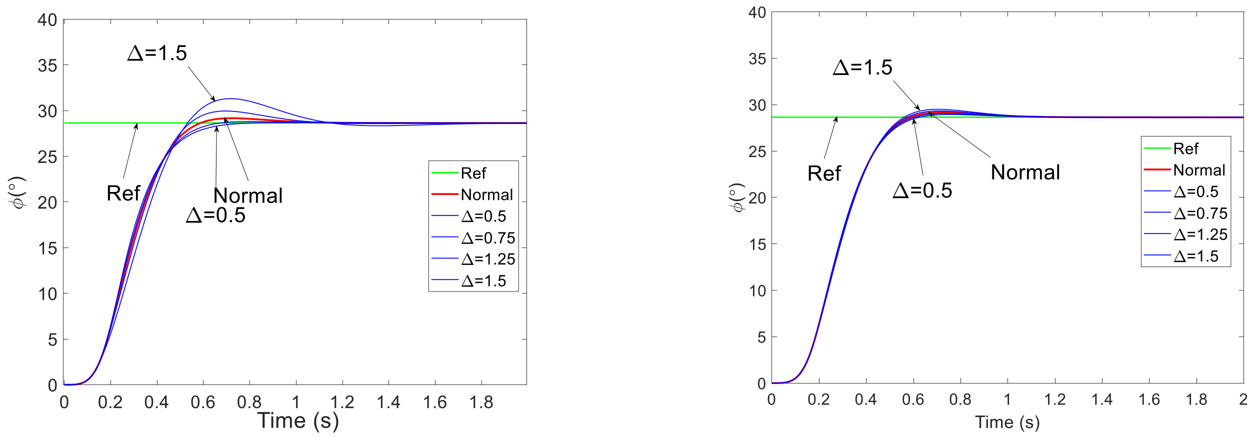

(a) PID (b) INDI

Fig. 6. The controller step response under different degrees of actuator modeling error.

3)、Robustness against disturbances

To validate the superiority of INDI in robustness, it is compared with traditionally tuned PID control as follows:

i. Pre-tune the parameters of PID to maintain a similar step response as the INDI controller, as shown in Fig. 5(b).

ii. After stabilizing the UAV system, apply an external disturbance at a certain time point and observe the response of INDI and PID to the disturbance.

iii. After conducting experiments with PID and INDI separately, the experimental results are displayed in Fig. 7. As shown in Fig. 7, at approximately 4 seconds, an external torque disturbance with a duration of 0.16 seconds is applied to the UAV, which simulates its response to adverse external disturbances such as impact or drag. The results indicate that despite both the proposed INDI controller and the PID controller having the same step response, the overall error of the former is significantly smaller than that of the latter when subjected to disturbances. This confirms the disturbance rejection of INDI.

Actually, due to its insensitivity to model information, INDI can effectively handle adverse effects caused by model mismatches, such as deviations in the UAV's center of gravity position, inaccuracies in rotor thrust and torque coefficients, and other factors.

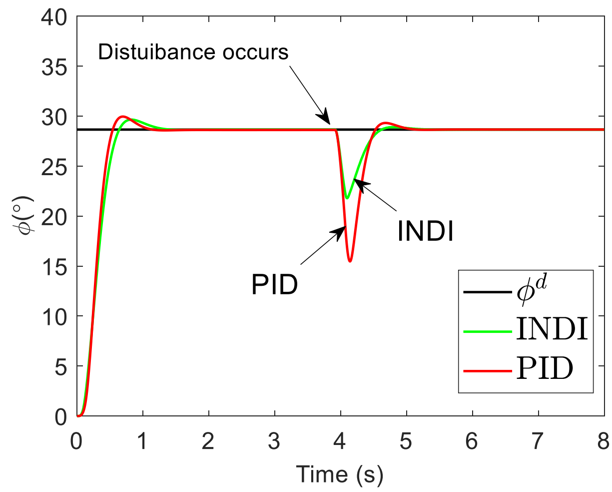

Fig. 7. Disturbance rejection response of INDI and PID.

4)、Robustness against Actuator modeling error

The relationship between the real execution efficiency $\bar{P}$ and the theoretical execution efficiency P of the actuator is added to satisfy this relationship $\bar{P} = \Delta \cdot P$

In this experiment, we simulate different Δ values to study the angle step response of INDI controller and PID controller. It can be seen from the results of Fig. 6 that the proposed INDI controller performs better than PID, which is reflected in the different delta values. The step response effect of INDI is better, which is close to that when Δ= 1, on the contrary, PID controller fails to do this.

5)、Robustness against model mismatch

During actual flight, the static parameters of the UAV may not be entirely accurate, including errors in the moment of inertia, lift coefficient of the propellers, and mass. These inaccuracies can negatively affect system stability. The INDI controller addresses this by measuring system dynamics in real time to detect and correct these errors.

Experimental conditions:

i. Set a step response of one radian and test the response time, overshoot, and steady-state error for both INDI and PID control.

ii. Change the model parameters, such as the UAV's mass, the lift coefficient of the propellers, and the moment of inertia, and repeat the experiment in i.

As shown in TABLE III, We can see that increasing or decreasing the values of mass and torque coefficient c_M does not cause significant experimental differences.

TABLE III
PERFORMANCE IN HANDLING MODEL MISMATCH

	Step response first reaching the target time [s]		Overshoot value [deg]		steady-state error [deg]	
	INDI	PID	INDI	PID	INDI	PID
Normal	0.632	0.528	1.00	1.29	0.00	0.03
+30% mass	0.632	0.528	1.00	1.29	0.00	0.03
-30% mass	0.632	0.528	1.00	1.29	0.00	0.03
+30% c_T	0.626	0.510	1.00	1.41	0.00	0.03
-30% c_T	0.646	0.554	0.99	1.25	0.00	0.03
+30% Jx	0.641	0.542	0.99	1.24	0.00	0.03
-30% Jx	0.622	0.508	1.01	1.35	0.00	0.04
+30% c_M	0.632	0.528	1.00	1.29	0.00	0.03
-30% c_M	0.632	0.528	1.00	1.29	0.00	0.03

This can be understood from (1), where attitude is directly related to the moment of inertia and not to mass, and the torque co-efficient affects the Z-axis angle without influencing the roll/pitch axis control performance.

However, in the experiments with the lift coefficient c_T and the moment of inertia Jx, PID reaches the target value faster than INDI for the first time, but it exhibits higher overshoot and instability when facing model mismatches.

This further confirms the robustness of INDI in handling model mismatches. Even in the presence of more complex nonlinear conditions, the INDI controller consistently exhibits superior robustness.

B. Real-world Experiments

We have assembled a quadcopter unmanned aerial vehicle (UAV), utilizing a custom-designed flight controller based on STM32F411. The motors utilized are EMAX-2205-2600kv, and the Electronic Speed Controllers (ESCs) are Skywalker 20A ESCs with 5045 2-blade propellers.

The motion control frequency is set at 200Hz, while the highest update frequency of the IMU sensor reaches 200Hz. The update frequency of the motor speed sensor is 400Hz. To achieve better control performance, the control frequency of the INDI inner loop is set at 400Hz.

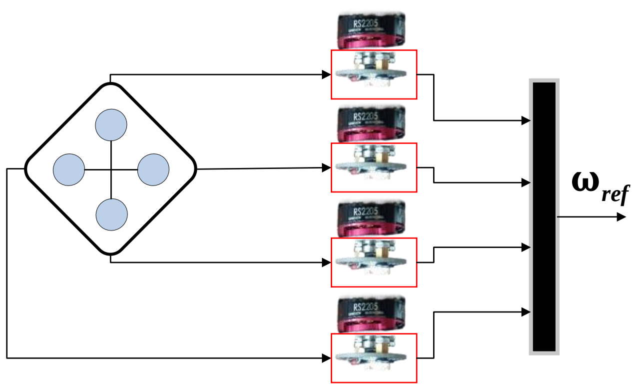

Fig. 8. Speed measurement of motor and magnetic encoder. Note a circular radial magnet attached to the bottom of the rotor.

Rotor speed data is obtained from the MT6701 magnetic encoder chip and filtered through a low-pass filter to eliminate high-frequency errors. Similarly, attitude data from the IMU also needs to be filtered using a low-pass filter with the same cutoff frequency to ensure consistency in the current system state data. Otherwise, this could lead to system oscillations.

1)、Angle tracking response

In actual control, both INDI and PID exhibit good attitude-tracking performance in Fig. 8. The main difference between the two lies in their robustness.

2)、Robustness against disturbances

During roll angle stabilization, a fixed roll torque is applied to the UAV. To ensure consistency in testing, a short-duration roll angle command is given to the UAV to simulate an external disturbance. This test is conducted on both the INDI and PID controllers for verification.

We observed that the maximum error value for INDI in disturbance rejection is approximately 26 degrees, which is less than PID's 42 degrees. Additionally, the recovery time for INDI is shorter than that of PID. Because INDI directly measures acceleration to correct errors, whereas PID relies on error integration to compensate for disturbances. The integrator gain in PID is limited by the stability requirements of the PID controller. Therefore, when designing a PID controller, a trade-off must be made between stability and disturbance rejection.

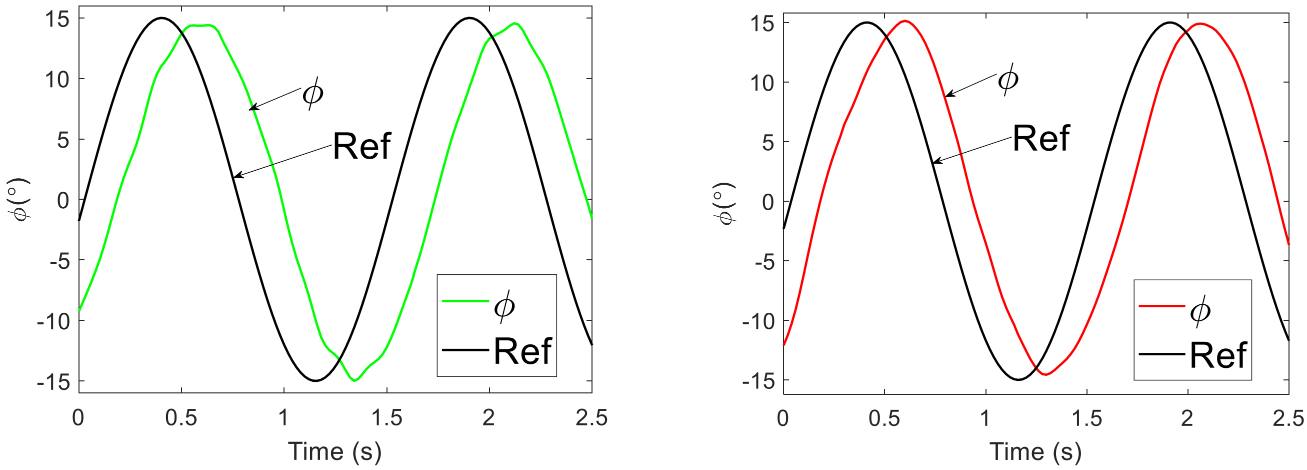

(a) INDI (b) PID

Fig.9. Attitude tracking response of the INDI&PID controller

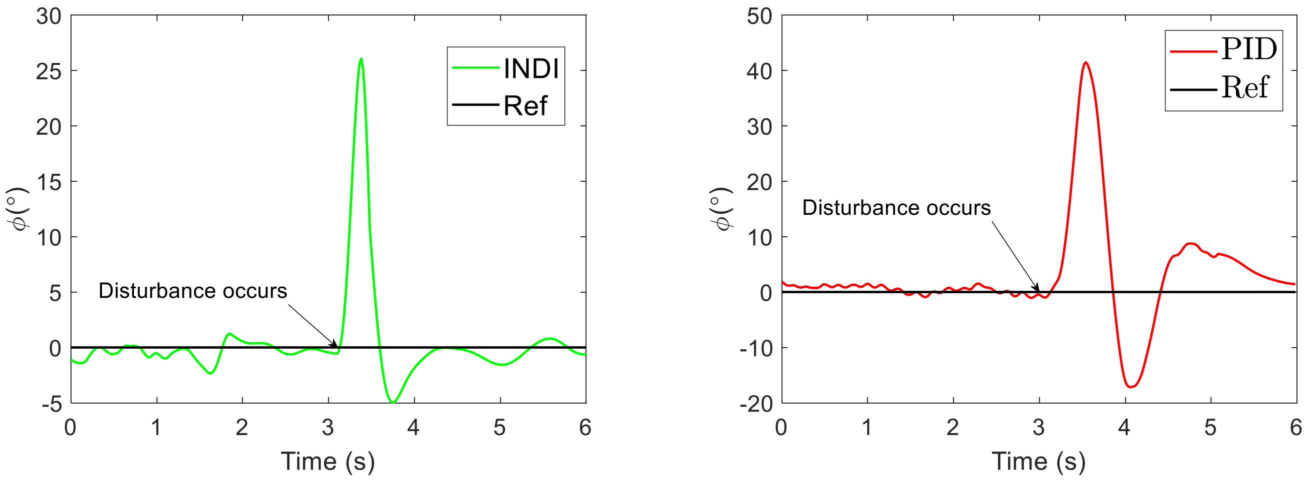

(a) INDI (b) PID

Fig. 10. Disturbance rejection response of INDI and PID

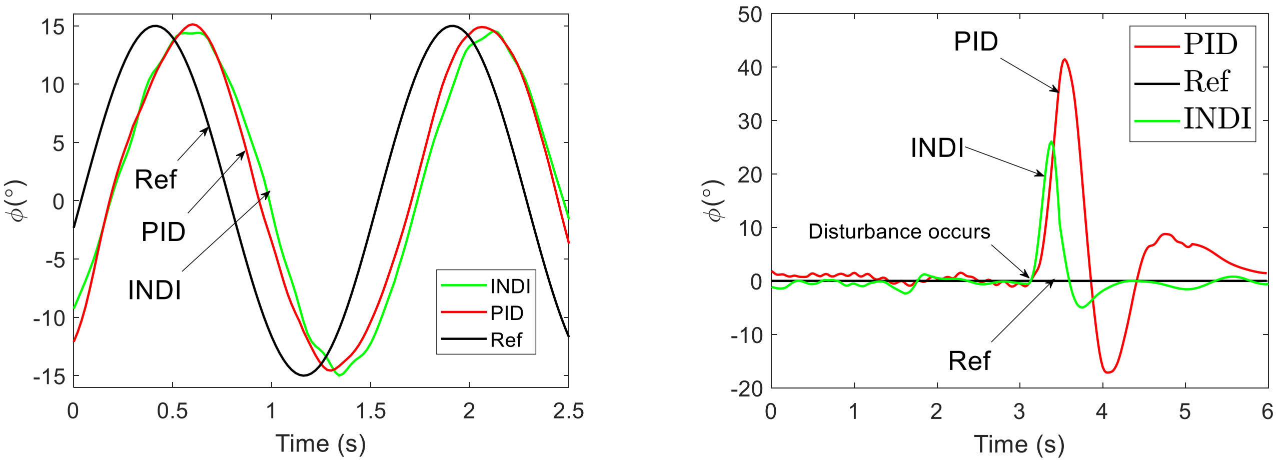

(a) Comparison of Attitude tracking response (b) Comparison of Disturbance rejection response

Fig. 11. Comparison of the effects of INDI and PID methods

V. CONCLUSION

This article proposes a strategy that applies NDI to the outer loop controller, and INDI to the inner loop controller for quadcopter UAV control, which counteracts uncertainties caused by model mismatches and improves system robustness. The effectiveness of the proposed controller is validated through both simulations and experiments. Comparative tests confirm that INDI has better disturbance rejection performance compared to traditional PID, with at least twice the effectiveness. A magnetic encoder was designed for closed-loop speed control, improving control accuracy. Compared to PID controllers, INDI controllers offer better robustness but at the cost of increased hardware expenses and higher computational complexity.

Future Work

While this study demonstrates the effectiveness and robustness of the proposed INDI-based control framework for quadcopter UAVs, several areas remain open for further investigation and improvement:

1). Optimization of Computational Efficiency

The INDI controller, while offering superior robustness, incurs higher computational complexity compared to traditional PID controllers. Future research could focus on developing more efficient algorithms or hardware acceleration techniques, such as leveraging field-programmable gate arrays (FPGAs) or parallel computing, to reduce computational overhead without compromising control performance.

2). Application to Multi-Agent Systems

Extending the proposed control framework to multi-agent UAV systems, such as drone swarms, presents an exciting research avenue. The scalability of the INDI controller and its ability to handle inter-agent interactions and communication delays warrant detailed exploration.

3). Integration of Advanced Sensors and Data Fusion

Incorporating advanced sensing technologies, such as LiDAR, visual odometry, or inertial measurement units (IMUs), and utilizing data fusion techniques could further enhance enhance the INDI controller's performance in complex, real-world environments.

By addressing these challenges, future research could significantly advance the applicability and effectiveness of INDI-based control systems in UAV and other robotics applications.

REFERENCES

[1] G. Loianno and D. Scaramuzza, "Special issue on future challenges and opportunities in vision-based drone navigation, " J. Field Robot., vol. 37, no. 4, pp. 495–496, 2020.

[2] S. Rajendran and S. Srinivas, "Air taxi service for urban mobility: A critical review of recent developments, future challenges, and opportunities, " Transp. Res. E, Logistics Transp. Rev., vol. 143, 102090, 2020.

[3] Bouabdallah S, Noth A, Siegwart R. "PID vs LQ control techniques applied to an indoor micro quadrotor, " 2004 IEEE/RSJ international conference on intelligent robots and systems (IROS) (IEEE Cat. No.04CH37566). 2004; Sendai, Japan. pp. 2451–2456.

[4] H. Liu, G. Lu, and Y. Zhong, "Robust LQR Attitude Control of a 3-DOF Laboratory Helicopter for Aggressive Maneuvers," IEEE Transactions on Industrial Electronics, vol. 60, no. 10, pp. 4627-4636, 2013

[5] Renbo Qing, Xiaoming Tang, Hua Huang and Yongzhen Cao. "An MPC Method for Trajectory Tracking of Unmanned Vehicle with LMI-Constrained Unscented Kalman Filter," IAENG International Journal of Computer Science. vol. 51, no.4, pp. 447-462, 2024.

[6] Li C, Jing H, Bao JD, et al. "Robust H_∞ fault tolerant control for quadrotor attitude regulation, "Proc Inst Mech Eng Part I: J Syst Control Eng. vol. 232, no. 10, pp. 1302–13, 2018.

[7] N. Seyed Gogani, V. Behnamgol, S. M. Hakimi, G. Derakhshan. "Finite Time Back Stepping Supper Twisting Controller Design for a Quadrotor," Engineering Letters. vol. 30, no. 2, pp. 674-680, 2022.

[8] Garcı´a O, Ordaz P, Santos-Sa´ nchez OJ, et al. "Backstepping and robust control for a quadrotor in outdoors environments: an experimental approach, " IEEE Access, vol. 7, pp. 40636–40648, 2019.

[9] Almakhles DJ. "Robust backstepping sliding mode control for a quadrotor trajectory tracking application," IEEE Access, vol. 8, pp. 5515–5525, 2020.

[10] Labbadi M, Cherkaoui M. "Robust adaptive nonsingular fast terminal sliding-mode tracking control for an uncertain quadrotor UAV subjected to disturbances," ISA Trans, vol. 99, pp. 290–304, 2019.

[11] S. Sun, A. Romero, P. Foehn, E. Kaufmann and D. Scaramuzza, "A Comparative Study of Nonlinear MPC and Differential-Flatness-Based Control for Quadrotor Agile Flight," in IEEE Transactions on Robotics, vol. 38, no. 6, pp. 3357-3373, 2022.

[12] Kaufmann, E., Bauersfeld, L., Loquercio, A. et al. "Champion-level drone racing using deep reinforcement learning," Nature, vol. 620, pp. 982–987, 2023.

[13] Z. Zhang, X. Li, L. Zhang and X. Zhao, "ANN-NDI-based Quadrotor UAV Large-Angle Maneuver Attitude Controller Design," 2023 IEEE International Conference on Mechatronics and Automation, ICMA 2023, 2023, Harbin, Heilongjiang, China, pp. 1996-2001.

[14] da Costa, R., Chu, Q., and Mulder, J., "Reentry Flight Controller Design Using Nonlinear Dynamic Inversion," Journal of Spacecraft and Rockets, vol. 40, no. 1, pp. 64-71, 2003.

[15] E.J.Smeur, Q.Chu, and G.C.deCroon, "Adaptive incremental nonlinear dynamic inversion for attitude control of micro air vehicles," J.Guid., Control, Dyn., vol. 39, no. 3, pp. 450-461, 2016

[16] Saldiran, Emre & Inalhan, Gokhan. "Incremental Nonlinear Dynamic Inversion-Based Trajectory Tracking Controller for an Agile Quadrotor: Design, Analysis, and Flight Tests Results, " In: Control of Autonomous Aerial Vehicles: Advances in Autopilot Design for Civilian UAVs, Cham, vol. Part F1768, pp. 195-230, 2023

[17] Cakiroglu, Can and Van Kampen, Erik-Jan and Chu, Q.P. "Robust incremental nonlinear dynamic inversion control using angular accelerometer feedback," In: 2018 AIAA Guidance, Navigation, and Control Conference, 2018, AIAA SciTech Forum, Florida, pp. 1128.

[18] Luo, F., Zhang, J., Jiang, B. "Robustness Analysis of Two Advanced Flight Control Laws: NDI and INDI, " In: Proceedings of the 5th China Aeronautical Science and Technology Conference. Lecture Notes in Electrical Engineering, vol. 821, 2022, Springer, Singapore, pp. 660-668.

[19] Q. Zhang, M. Fu, C. Zhai, S. Wang, K. Ning and M. Wang, "Incremental Nonlinear Dynamic Inversion Control for Quadrotor UAV With an Angular Accelerometer," 42nd Chinese Control Conference (CCC) 2023, 2023, Tianjin, China, pp. 657-662.

[20] Jiesong Yang, Zhihao Cai, Jiang Zhao, Zexin Wang, Yongfei Ding, Yingxun Wang, "INDI-based aggressive quadrotor flight control with position and attitude constraints," Robotics and Autonomous Systems, vol. 159, 104292, 2023.

[21] E. Tal and S. Karaman, "Accurate Tracking of Aggressive Quadrotor Trajectories Using Incremental Nonlinear Dynamic Inversion and Differential Flatness," in IEEE Transactions on Control Systems Technology, vol. 29, no. 3, pp. 1203-1218, 2021,

[22] Smeur EJJ, de Croon GCHE, Chu Q. "Cascaded incremental nonlinear dynamic inversion for MAV disturbance rejection, " Control Engineering Practice, vol. 73, pp. 79-90, 2017.

[23] S. Sun, X. Wang, Q. Chu and C. d. Visser, "Incremental Nonlinear Fault-Tolerant Control of a Quadrotor with Complete Loss of Two Opposing Rotors," in IEEE Transactions on Robotics, vol. 37, no. 1, pp. 116-130, 2021.

[24] Wang, Xuerui and Van Kampen, Erik-Jan and Chu, Qiping and Lu, Peng, " Stability Analysis for Incremental Nonlinear Dynamic Inversion Control, " Journal of Guidance, Control, and Dynamics, vol. 42, no.5, pp. 1116-1129, 2019.

[25] Almido Haryanto Ginting, Oyas Wahyunggoro, and Adha Imam Cahyadi, "Robust Proportional-Derivative Control on SO(3) to Compensate The Unknown Center of Gravity of Quadrotor," Engineering Letters. vol.28, no.2, pp. 359-370, 2020.